ISSN 2072-5981

Magnetic Resonance in Solids

Electronic Journal

Volume ***18,***
Issue ***2***
Paper No ***16204,***
1-6 pages
2016

http://mrsej.kpfu.ru
http://mrsej.ksu.ru

Established and published by Kazan University
Sponsored by International Society of Magnetic
Resonance (ISMAR)
Registered by Russian Federation Committee on Press,
August 2, 1996
First Issue was appeared at July 25, 1997

"***Magnetic Resonance in Solids. Electronic Journal***" (**MRS*ej***) is a peer-reviewed, all electronic journal, publishing articles which meet the highest standards of scientific quality in the field of basic research of a magnetic resonance in solids and related phenomena. **MRS*ej*** is free for the authors (no page charges) as well as for the readers (no subscription fee). The language of **MRS*ej*** is English. All exchanges of information will take place via Internet. Articles are submitted in electronic form and the refereeing process uses electronic mail. All accepted articles are immediately published by being made publicly available by Internet (http://**MRS*ej***.kpfu.ru).

---

[*] In Kazan University the Electron Paramagnetic Resonance (EPR) was discovered by Zavoisky E.K. in 1944.

Magnetic properties of powders $LiTbF_4$ and TbF_3[†]

E.M. Alakshin[1], A.V. Klochkov[1], S.L. Korableva[1], V.V. Kuzmin[1], D.S. Nuzhina[1,*],
I.V. Romanova[1], A.V. Savinkov[1], M.S. Tagirov[1,2]
[1]Kazan Federal University, Kremlevskaya 18, Kazan 420008, Russia
[2]Institut of Perspective Research, TAS, L. Bulachnaya 36a, Kazan 420111, Russia
E-mail: nuzh.darya@gmail.com

(Received December 10, 2016; accepted December 17, 2016)

Samples $LiTbF_4$ and TbF_3 were synthesized by modified methods of colloidal chemistry. The magnetization of these samples was measured in the external magnetic field at 100 Oe and 1 T and in temperature range 2-300 K. Temperatures of phase transition to the magnetic ordering dipolar ferromagnet state were determined for synthesized samples.

PACS: 75.50.-y, 75.90+w, 81.10-h

Keywords: synthesis, magnetization, Curie temperature

1. Introduction

The complex fluorides $LiReF_4$ (Re is rare earth ion) represent a class of crystal materials used as model objects in physics of dipolar magnets. Crystals of rare-earth tetrafluoride compounds with a controlled size, shape, structure and surface have unique optical, electronic, magnetic and catalytic properties important for practical applications [1]. The $LiTbF_4$ crystal has a scheelite ($CaWO_4$) structure with the space group C_{4h}^{6} [2] and TbF_3 crystallizes in orthorhombic D_{2h}^{16} space group [3]. Trifluorides exhibit distinct magnetic properties at low temperatures and they are of interest as model systems for the theoretical study of magnetic ordering in condition of competition between the dipole-dipole and exchange interactions [4].

Measurements of magnetic *DC*-susceptibility in $LiTbF_4$ single crystals showed that $LiTbF_4$ is the dipole Ising dielectric ferromagnet at temperatures below the $T_c = 2.89\,\mathrm{K}$ [5,6]. Magnetic moments of Tb^{3+} are ordered along the *c*-easy axis at $T < T_c$. The TbF_3 is also a dipolar ferromagnet, as it was found in the magnetization measurements [4]. The phase transition in TbF_3 single crystal from the paramagnetic to the ferromagnetic state occurs at temperatures below $T_c = 3.95\,\mathrm{K}$ [4]. At low temperatures ($T < T_c$) magnetic moments of ions Tb^{3+} ($\sim 9\ \mu\mathrm{B}$) are ordered in two magnetically non-equivalent sublattices in the crystallographic *ac* plane at angles $\varphi = \pm 28^\circ$ to the *a*-axis. Due to large values of the magnetic moments, the magnetic ordering is induced mainly by classical dipole-dipole interaction between the terbium ions, which dominates the magnetic exchange interaction.

The tetrafluorides $LiTbF_4$, $LiDyF_4$, $LiHoF_4$ and $LiErF_4$ have been the subject of intensive studies by NMR and EPR. The nuclear magnetic resonance rotation spectra were observed and contributions to the local magnetic fields from the dipole and the transferred hyperfine interactions were distinguished [7]. The fluorine and lithium NMR line shifts have been measured [8] in the temperature range from 300 to 1.3 K and in the fields up to 40 kG for $LiTbF_4$, $LiHoF_4$. Angular dependences of fluorine NMR spectra have been observed in the external magnetic field,

---

[†] This paper material was selected at XIX International Youth Scientific School "Actual problems of magnetic resonance and its application", Kazan, 24 – 28 October 2016. The paper was recommended to publication in our journal and it is published after additional MRSej reviewing.

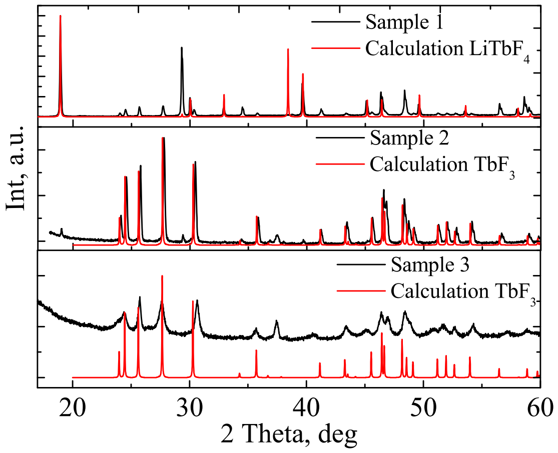

Figure 1. XRD patterns of samples 1-3.

Table 1. Characteristic size of samples 1-3 obtained by Photocor Complex.

Sample	Characteristic size (diameter)
$LiTbF_4$(79.9%)+TbF_3(20%)	20 mkm
$LiTbF_4$(6.9%)+TbF_3(81.2%)	1.5 mkm
TbF_3	585 nm

the constants of transferred hyperfine interaction and the corrected set of crystal field parameters for the Tb^{3+} ions in $LiTbF_4$ have been determined determined [9]. The EPR investigations were done in $LiTbF_4$, $LiHoF_4$ and $LiErF_4$ single crystals at submillimeter wavelength. The temperature and angle dependencies of resonance line width were studied and described by the dipole dipole interactions of Re^{3+} ions and local fields around Re^{3+} ions [10]. The hyperfine structure of EPR spectra of Tb^{3+} ions was considered [11], the strong dipole interactions give a strong line broadening, but if the applied magnetic field is high enough to saturate the magnetization, each electron becomes in the same magnetic surrounding, so the line narrowing one can observe.

Influence of nanoparticle size on the magnetic, optical and electronic properties of the fluorides is one of the fundamental problems in the physics of the rare-earth compounds and fundamental physics. Nanoparticles of DyF_3 were synthesized by the colloidal chemistry methods [12]. The influence of the microwave-assisted hydrothermal treatment on magnetic properties and structure of PrF_3 and LaF_3 nanoparticles was investigated by XRD, TEM, NMR and EPR [12–21]. In this paper we present the few synthesis technique for TbF_3 and $LiTbF_4$ materials. Magnetic and structure properties of the TbF_3 and $LiTbF_4$ powders are investigated by DC-susceptibility measurements.

2. Syntesis of micro- and nano-sized powders

The synthesis of $LiTbF_4$ is complex procedure [1,22]. The method of synthesis with trifluroacetate precursors is chemically aggressive, the methods of hydrothermal synthesis and thermal decomposition demand high temperatures and high pressure in autoclave [22–28].

The samples of $LiTbF_4$ were synthesized using following techniques:

Sample 1: $LiNO_3(aq)+Tb(NO_3)_3+NH_4(aq)\rightarrow \text{powder} \xrightarrow{400^\circ,4h} LiTbF_4(s)+TbF_3(s)$.

Sample 2: $LiOH(aq)+Tb(NO_3)_3+NH_4(aq)\rightarrow \text{powder} \xrightarrow{400^\circ,4h,CF_4} LiTbF_4(s)+TbF_3(s)$.

The TbF_3 nanoparticles were synthesized using standard technologies [10,11].

Sample 3: $Tb(NO_3)_3+NaF(aq)\rightarrow TbF_3(s)+NaNO_3(aq)$.

The X-ray analysis was carried out by an automatic X-ray diffractometer Bruker D8 Advance with Cu Kα radiation ($\lambda = 1.5418$ Å) at Bragg-Brentano geometry. Result of the X-ray analysis of synthesized samples is shown in Fig. 1. Phase ratio of $LiTbF_4$ and TbF_3 in samples 1-2 was determined using MAUD software [29].

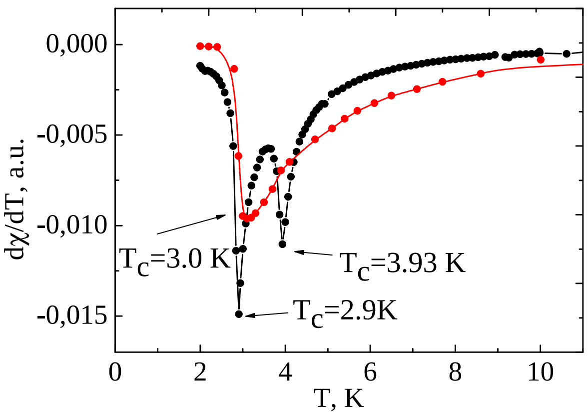

Figure 2. Derivatives of magnetic susceptibility versus temperature for $LiTbF_4$(79.9±0.7%) +TbF_3(20.0±0.5%) powders (black points) and $LiTbF_4$ single crystal (red points) [30] in external magnetic field 100 Oe.

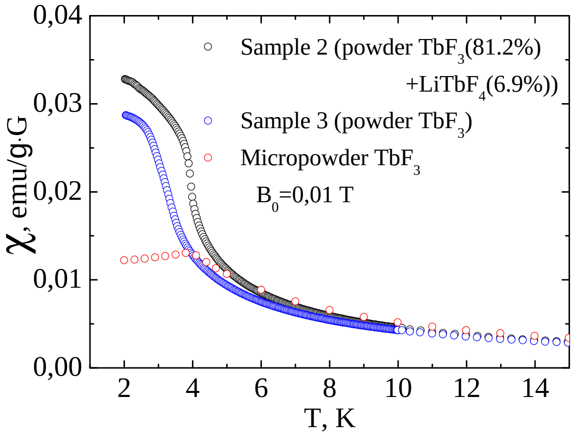

Figure 3. Temperature dependencies of magnetic susceptibility for sample 2 (TbF_3(81.2±0.4%) +$LiTbF_4$(6.9±0.1%)) (black points), sample 3 (blue points) and micropowder TbF_3 (red points) in external magnetic field 100 Oe.

The chemical composition of the synthesized samples is:

Sample 1 - $LiTbF_4$(79.9±0.7%)+TbF_3(20.0±0.5%),

Sample 2 - TbF_3 (81.2±0.4%) + $LiTbF_4$(6.9±0.1%)+$LiNO_3$ H_2O(11.9±1.1%),

Sample 3 - TbF_3(99±1%).

Particle size was preliminary determined using the dynamic and static light scattering spectrometer for registration nanoparticles size and composition Photocor Complex (table 1). Such big particles size probably can be explained by agglomeration of particles in the solution.

3. Study of magnetic properties, discussion and results

The temperature dependencies of magnetic susceptibility for all synthesized samples were measured by PPMS-9 System (Quantum Design Inc.) at applied magnetic fields 100 Oe and 1 T in temperature range 2-300 K. The derivative of magnetic susceptibility versus temperature for the sample 1 is shown in Fig. 2. There are two phase transitions at temperatures $T = 2.9\,\mathrm{K}$ and $T = 3.93\,\mathrm{K}$, which correspond to the Curie temperature of the transitions to the ferromagnetic state for $LiTbF_4$ and TbF_3 single crystals, respectively. The red curve in Fig. 2 represents the dependence for single crystal $LiTbF_4$ in the magnetic field $\mathbf{B}\|c$ [30]. The total magnetization would be reduced, because all possible particles directions in external magnetic field are equivalent in powder.

The temperature dependences of magnetic susceptibility for the sample 2 (black points) and sample 3 (blue points) are shown in Fig. 3. There are no clear evidence of transitions to a magnetically ordered state for TbF_3 or $LiTbF_4$. This may be due to the fact that the ordering of magnetic domains happens not simultaneously.

Fig. 4 shows the measured temperature dependence of the magnetic susceptibility of the powder samples 3 (TbF_3 powder). The temperature dependences of the magnetic susceptibility of single crystal TbF_3 demonstrate a strong anisotropy (the black points correspond to the $\chi\|a$ direction, the pink points correspond to the $\chi\|b$ direction, the green points correspond to the $\chi\|c$ direction) [4].

The magnetic susceptibility of the powder can be described by $\chi_\mathrm{p} = (\chi_\mathrm{a}+\chi_\mathrm{b}+\chi_\mathrm{c})/3$, where χ_a, χ_b, χ_c are magnetic susceptibilities along the axes a, b, c due to the symmetry of the crystal lattice. These calculations do not well fit the experimental results, because the size and shape of the particles were not taken into account. The crystal field and local magnetic field at the rare-earth ions located near the surface of nanoparticles are also different from ones in the bulk.

Theoretical calculation of the magnetic susceptibility of LiTbF$_4$ is shown on Fig. 5 (red line). Here all possible orientations of the external magnetic field along the crystallographic c-axis of the nanoparticles were taken into account. The shape of the nanoparticles assumed spherical, the summation carried on sphere 360°. Therefore the magnetization along c-axis [30]:

$$M_z = B_z \left[\lambda \left(\frac{\tanh(\delta/2k_\mathrm{B}T_\mathrm{c})}{\tanh(\delta/2k_\mathrm{B}T)} - 1 \right) + N \right]^{-1},$$

where λ is molecular field constant ($\lambda = 5.23 \pm 0.56$), δ is initial splitting in the ground state quasidoublet ($\delta = 1\,\mathrm{cm}^{-1}$) of basic $^7F_6$ multiplet, N is demagnetization factor ($N = 4\pi/3$), B_z is external magnetic field, T_c is the Curie temperature.

The measured temperature dependences of sample 1 and single crystal LiTbF$_4$ at $\mathbf{B}_0 \| a$ and $\mathbf{B}_0 \| c$ in external magnetic field ($B_0 = 1\,\mathrm{T}$) are presented in the Fig. 5.

The curve 5 in Fig. 5 shows the calculations which take into account all possible crystallographic c-axis of the particle orientations with respect to external magnetic field. The discrepancy between the theoretical calculations and experimental data can also be explained by the fact that the calculation has not considered TbF$_3$ presence, nanoparticles shape and size.

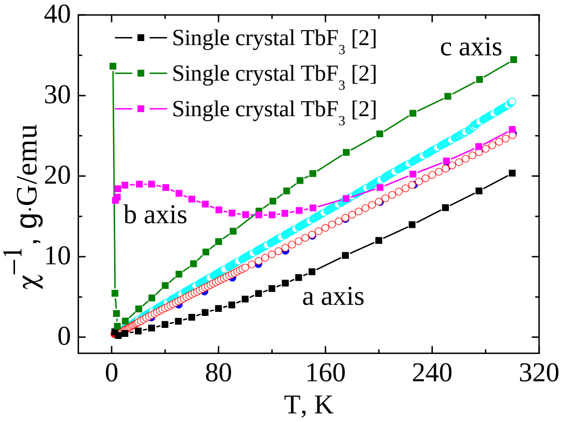

Figure 4. Temperature dependencies of magnetic susceptibility for sample 3 (cyan points), micropowder TbF$_3$ (red points), single crystal TbF$_3$ in different directions of crystal lattice [4] and calculation magnetic susceptibility of the powder TbF$_3$ [4] (blue points).

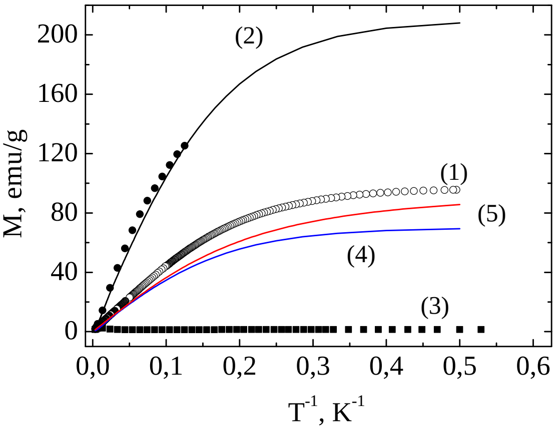

Figure 5. The temperature dependence of the magnetization for sample 1 (LiTbF$_4$(79.9±0.7%) +TbF$_3$(20.0±0.5%)) (curve 1, black points), LiTbF$_4$ single crystal along the crystallographic c-axis (curve 2, black points) [30] and a,b-axis (curve 3, black points) [30]; Theoretical calculations of the magnetization for LiTbF$_4$ single crystal along c-axis (curve 2, black line) [30], calculations of the magnetization of LiTbF$_4$ (curves 4, 5) at $B = 1\,\mathrm{T}$.

Curve 4 (blue line) in Fig. 5 shows the calculations which take into account the following considerations: magnetic Tb^{3+} moments in LiTbF$_4$ single crystal are arranged along c-axis of the crystal lattice, the magnetization along the a-axis and b-axis is almost zero. Distribution of the c-axis orientations related to the direction of the external magnetic field is of the same probability. Thus, the magnetization along the a and b-axis can be neglected and the total magnetization can be estimated as $M = M_z/3$. The unusual behavior of the magnetization and magnetic susceptibilities in micro- and nano-sized powders LiTbF$_4$ and TbF$_3$ will be studied in detail later.

4. Conclusion

The samples of the rare-earth fluorides were synthesized. Crystallographic structure of the synthesized samples has been identified by the X-ray diffraction, magnetic properties of the powders mainly agree with the $LiTbF_4$ magnetic properties in the bulk. However improvement of the synthesis method is needed because the undesirable TbF_3 phase (∼20%) was found.

Acknowledgments

The work is performed according to the Russian Government Program of Competitive Growth of Kazan Federal University, partly supported by the Russian Foundation for Basic Research (Project No.16-32-60155 mol_a_dk). The magnetic measurements were carried out at the Federal Center of Shared Facilities of Kazan Federal University. Authors thank Shustov V.A. for analysis XRD patterns.

References

1. Du Y.-P., Zhang Y.-W., Sun L.-D., Yan C.-H., *Dalton Transactions* **40**, 8574 (2009).

2. Weber M. J., Morgret R., Leung S. Y., Griffin J. A., Gabbe D., Linz A., *Journal of Applied Physics* **49**, 3464 (1978).

3. Holmes L., Guggenheim H. J., Hull G. W., *Solid State Communications* **8**, 2005 (1970).

4. Holmes L., Guggenheim H., *Journal de Physique Colloques* **32**, 501 (1971).

5. Holmes L. M., Johansson T., Guggenheim H. J., *Solid State Communications* **12**, 993 (1973).

6. Als-Nielsen J., Holmes L. M., Larsen F. K., Guggenheim H. J., *Physical Review B* **12**, 191 (1975).

7. Hansen P. E., Nevald R., *Physical Review B* **16**, 146 (1977).

8. Nevald R., Hansen P. E., *Physical Review B* **18**, 4626 (1978).

9. Romanova I. V., Egorov A. V., Korableva S. L., Malkin B. Z., Tagirov M. S., *Journal of Physics: Conference Series* **324** (2011).

10. Magario J., Tuchendler J., Beauvillain P., Laursen I., *Physical Review B* **21**, 18 (1980).

11. de Groot P., Leempoels F., Witters J., Herlach F., Laursen I., *Solid State Communications* **37**, 681 (1981).

12. Alakshin E. M., Klochkov A. V., Kondratyeva E. I., Korableva S. L., Kiiamov A. G., Nuzhina D. S., Stanislavovas A. A., Tagirov M. S., Zakharov M. Y., Kodjikian S., *Journal of Nanomaterials* **2016**, 7148307 (2016).

13. Tagirov M. S., Alakshin E. M., Gazizulin R. R., Egorov A. V., Klochkov A. V., Korableva S. L., Kuzmin V. V., Nizamutdinov A. S., Kono K., Nakao A., Gubaidullin A., *Journal of Low Temperature Physics* **162**, 645 (2011).

14. Alakshin E. M., Aleksandrov A. S., Egorov A. V., Klochkov A. V., Korableva S. L., Tagirov M. S., *JETP Letters* **94**, 240 (2011).

15. Alakshin E. M., Blokhin D. S., Sabitova A. M., Klochkov A. V., Klochkov V. V., Kono K., Korableva S. L., Tagirov M. S., *JETP Letters* **96**, 181 (2012).

16. Alakshin E. M., Gazizulin R. R., Klochkov A. V., Korableva S. L., Kuzmin V. V., Sabitova A. M., Safin T. R., Safiullin K. R., Tagirov M. S., *JETP Letters* **97**, 579 (2013).

17. Pudovkin M. S., Korableva S. L., Krasheninnicova A. O., Nizamutdinov A. S., Semashko V. V., Zelenihin P. V., Alakshin E. M., Nevzorova T. A., *Journal of Physics: Conference Series* **560** (2014).

18. Alakshin E. M., Gazizulin R. R., Klochkov A. V., Korableva S. L., Safin T. R., Safiullin K. R., Tagirov M. S., *Optics and Spectroscopy* **116**, 721 (2014).

19. Gazizulina A. M., Alakshin E. M., Baibekov E. I., Gazizulin R. R., Zakharov M. Y., Klochkov A. V., Korableva S. L., Tagirov M. S., *JETP Letters* **99**, 149 (2014).

20. Alakshin E. M., Gazizulin R. R., Gazizulina A. M., Klochkov A. V., Orlinskii S. B., Rodionov A. A., Safin T. R., Safiullin K. R., Tagirov M. S., Zakharov M. Y., *Low Temperature Physics* **41**, 47 (2015).

21. Alakshin E. M., Gizatullin B. I., Zakharov M. Y., Klochkov A. V., Salikhov T. M., Skirda V. D., Tagirov M. S., *Low Temperature Physics* **41**, 67 (2015).

22. Mahalingam V., Vetrone F., Naccache R., Speghini A., Capobianco J. A., *Advanced Materials* **21**, 4025 (2009).

23. Fedorov P. P., Kuznetsov S. V., Voronov V. V., Yarotskaya I. V., Arbenina V. V., *Russian Journal of Inorganic Chemistry* **53**, 1681 (2008).

24. Brinkmann J., Courths R., Hfner S., Guggenheim H. J., *Journal of Magnetism and Magnetic Materials* **6**, 279 (1977).

25. Lu C., Huang W., Ni Y., Xu Z., *Materials Research Bulletin* **46**, 216 (2011).

26. Chen S., Wang S., Zhang J., An L., *Journal of Nanoscience and Nanotechnology* **9**, 1942 (2009).

27. Li C., Lin J., *Journal of Materials Chemistry* **20**, 6831 (2010).

28. Joubert M. F., Jacquier B., Moncorg R., *Physical Review B* **28**, 3725 (1983).

29. Lutterotti L., *Nuclear Instruments and Methods in Physics Research, Section B: Beam Interactions with Materials and Atoms* **268**, 334 (2010).

30. Romanova I. V., Malkin B. Z., Mukhamedshin I. R., Suzuki H., Tagirov M. S., *Physics of the Solid State* **44**, 1544 (2002).